CLEAN
Soil Air Water



**Sabtanti Harimurti**[1,2]
**Anisa Ur Rahmah**[1]
**Abdul Aziz Omar**[1]
**Murugesan Thanapalan**[1]

[1]Department of Chemical Engineering, Universiti Teknologi PETRONAS, Bandar Seri Iskandar, Tronoh, Malaysia
[2]Faculty of Medicine and Health Science, Department of Pharmacy, University Muhammadiyah Yogyakarta, Yogyakarta, Indonesia

Research Article

# Kinetics of Methyldiethanolamine Mineralization by Using UV/$H_2O_2$ Process

The UV/$H_2O_2$ is one of the popular techniques in the advanced oxidation processes (AOPs) and has been applied in the wastewater treatment during recent two decades. UV exposure on the $H_2O_2$ generate highly reactive hydroxyl radicals ($OH^{\bullet}$), which are used to degrade organic contaminants through oxidation processes in wastewater. This present study involves the estimation of hydroxyl radical rate constants of methyldiethanolamine (MDEA) mineralization at different temperatures by using UV/$H_2O_2$ in aqueous solution. Laboratory experiments have been conducted and the profile of MDEA mineralization has been established. The hydroxyl radical rate constants and the activation energy of mineralization process have been calculated. The estimated hydroxyl rate constants and the activation energy are in good agreement with those reported in the literature.

**Keywords:** Activation energy; Alkanolamine; Hydroxyl radical rate constant; Oxidation process; Petrochemical industry

*Received:* March 19, 2012; *revised:* July 10, 2012; *accepted:* August 2, 2012

**DOI:** 10.1002/clen.201200121

## 1 Introduction

Methyldiethanolamine (MDEA) is one of the common alkanolamines, which is widely used in petrochemical industries namely, refineries, ammonia gas plant, and natural gas treatment plant, etc. Aqueous MDEA solutions are commonly used for the absorption/scrubbing of acidic gases ($CO_2$ and $H_2S$) from natural gas. MDEA is also used in the formulation of surfactants, emulsifiers, and fabric softeners, etc. During the processing of the above, high concentrations of MDEA in solutions are released in to the atmosphere in the form of wastewater/effluents, particularly during the periodic maintenance and cleaning of the contacting equipments (absorber and strippers). These effluents containing high concentration of MDEA must be treated before their release in to atmosphere. One of the well established technique known as advanced oxidation process (AOP) using Fenton's reagent has been used to degrade the alkanolamines present in the effluents. Fenton's reagent (a mixture of hydrogen peroxide with ferrous sulfate) has been used to degrade MEA [1], DEA [2], and DIPA [3]. Even though the Fenton's reagent is more effective to degrade, it will form sludge at particular pH conditions. Due to the limitation/disadvantages of Fenton's reagent, a different technique based on UV/$H_2O_2$ was used by Ariff [4] to degrade MEA in aqueous solution. The advantages of UV/$H_2O_2$ process are: no formation of sludge during the treatment, high ability to produce hydroxyl radicals and applicability of the process for a wide pH range.

During UV irradiation of $H_2O_2$, it is well known that a strongly oxidizing agent namely hydroxyl radicals ($^{\bullet}OH$) are formed in the solution and they have a very high oxidation potential to degrade many organic contaminants present in the wastewater/effluent stream [5–8]. As reported by Malik and Sanyal [9] and also by Muruganandham and Swaminathan [10], the UV/$H_2O_2$ process is effective for the decolorization of azo-dyes, whereas the degradation of 4-nitrophenol using UV/$H_2O_2$ was reported by Daneshvar et al. [11]. The degradation of phenol and chlorinated phenols using UV/$H_2O_2$ were also demonstrated by De et al. [12]. Lopez et al. [13] successfully degraded 4-chloro-3,5-dinitrobenzoic acid (CDNBA) in aqueous solution. Degradation and detoxification of formalin in wastewater using UV/$H_2O_2$ was reported by Kajitvichyanukul et al. [14]. Based on the advantages of UV/$H_2O_2$ process for the degradation of alkanolamines in the effluent stream, in this work it is proposed to use the combination of UV/$H_2O_2$ technique to degrade the simulated MDEA solution. In order to develop UV/$H_2O_2$ AOP for scale up and further commercial applications, the kinetics of the process, in particular, the knowledge of hydroxyl radical rate constants are essentially looked-for. Hence in the present work it is proposed to conduct experiments to verify MDEA mineralization profile and to formulate a kinetic model for the degradation of MDEA.

## 2 Materials and methods

### 2.1 Materials

Methyldiethanolamine (MDEA) (CAS no. 105-59-9), potassium permanganate ($KMnO_4$), sulfuric acid ($H_2SO_4$), and hydrogen peroxide ($H_2O_2$) were obtained from Merck (Germany). Sodium hydroxide (NaOH) was obtained from RM Chemicals (Malaysia).

**Correspondence:** Dr. M. Thanapalan, Departement of Chemical Engineering, Universiti Teknologi PETRONAS, Bandar Seri Iskandar, 31750 Tronoh, Perak Darul Ridzwan, Malaysia
**E-mail:** tmgesan_57@yahoo.com; murugesan@petreonas.com.my

**Abbreviations: MDEA,** methyldiethanolamine; **TOC,** total organic carbon

© 2013 WILEY-VCH Verlag GmbH & Co. KGaA, Weinheim

CLEAN Soil Air Water

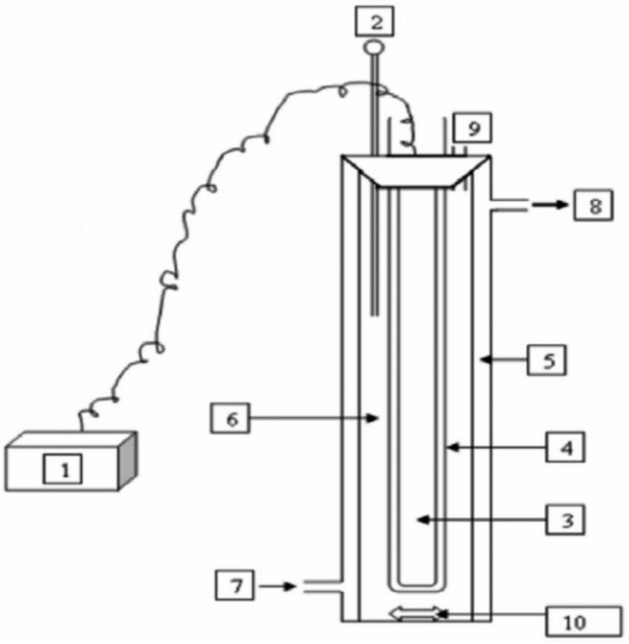


**Figure 1.** Scheme of the UV/$H_2O_2$ photoreactor. (1) Current–voltage control unit; (2) Thermometer; (3) UV lamp; (4) Quartz tube; (5) Jacket; (6) Reaction zone; (7) Water inlet; (8) Water outlet; (9) Sample port; and (10) Stirrer bar.

## 2.2 Methods

Methyldiethanolamine (MDEA) mineralization experiments were conducted in a 700 mL stirred jacketed glass reactor (Fig. 1) to monitor the degradation progress. A jacketed cylindrical borosilicate glass column of 14 inch height with 2 inch id was used as the reaction zone. The photo reactor was equipped with a low pressure Hg vapor lamp GPH295T5L (producing UV light at 254 nm was made in USA with serial no. EC90277), a voltage control unit, and an opening for collecting the samples. Aluminum foil was used to cover the photo reactor. For the degradation studies, a known concentration of amine solution was taken into the glass reactor and a required amount of $H_2O_2$ was added in to the reactor. The total volume (400 mL) includes the volume of amine solution and $H_2O_2$. The total volume (400 mL) is the volume, where the UV lamp totally immerses in the solution. The pH adjustment was made using 1 mol $L^{-1}$ NaOH/0.5 mol $L^{-1}$ $H_2SO_4$. The temperature of oxidation process was maintained by circulating water (at required temperature) through the jacket. During the process, samples were withdrawn from time to time to follow the mineralization process. The total organic carbon (TOC) of the samples were measured using TOC analyzer (Shimadzu TOC-$V_{CSH}$) and the $H_2O_2$ concentration was estimated by $KMnO_4$ titration [15]. In order to check the stability of MDEA at different pH ranges, experiments were conducted at three extreme conditions, i.e., at pH 3.0, 9.79, and 11. The estimated TOC values after 3 h were found to be nearly the same and it can be concluded that the MDEA is not affected by the change in pH of the solution. During the experiments, approximately 2–3 mL of the samples were withdrawn and diluted further for the estimation of TOC and unreacted $H_2O_2$. The range of variables covered in the present studies include: (i) four initial amine concentration (1000, 2000, 3000, and 4000 mg $L^{-1}$); (ii) five initial concentration of $H_2O_2$ (0.06, 0.09, 0.12, 0.19, and 0.22 mol $L^{-1}$); and (iii) four different temperatures (20, 30, 40, and 50°C).

# 3 Results and discussion

## 3.1 MDEA mineralization profile

The most common techniques for the generation of the strongly oxidizing hydroxyl radicals (•OH) are Fenton's reagent, combination of UV/$O_3$ or the combination of UV/$H_2O_2$. The present study involves the mineralization of MDEA by hydroxyl radical (•OH), which are generated by UV/$H_2O_2$ process. UV light and $H_2O_2$ can also be used independently to degrade organic contaminants in the wastewater [9, 12]. But for the case of MDEA mineralization, degradation occurs only when using the combination of UV with $H_2O_2$, i.e., mineralization occurs due to the formation of hydroxyl radical through the exposure of UV light to $H_2O_2$. For the present experiments, the intensity of UV lamp source was maintained at 12.06 mW $cm^{-2}$ and the irradiation was carried out for 3 h. Oxidation temperature was varied from 20 to 50°C. Based on our preliminary experiments [16], the optimum pH was found as 10.18 and hence the initial pH was adjusted to 10.18 for all the present experiments. The mineralization of MDEA also increased with an increase in $H_2O_2$ concentration up to 0.22 mol $L^{-1}$. Further increase in $H_2O_2$ concentration led to a decrease in the mineralization. Hence, to determine the kinetic constants of MDEA mineralization, the estimated optimum concentration of $H_2O_2$ (0.22 mol $L^{-1}$) with a pH of 10.18 were used for the present experiments. The estimated experimental reduction rates for MDEA, during the initial 30 min are presented in Tab. 1.

Figure 2 shows the profile of MDEA mineralization at different temperatures (20–50°C) and also at different initial concentrations of $H_2O_2$ (0–0.22 mol $L^{-1}$). The initial pH, initial concentration of contaminant, UV light intensity, and irradiation period were kept constant at 10.18, 2000 mg $L^{-1}$ (0.085 mol $L^{-1}$ organic carbon), 12.06 mW $cm^{-2}$ and 3 h, respectively. In the absence of $H_2O_2$, no/negligible mineralization was observed for all the temperatures, even with UV light irradiation for 3 h. Similarly, in the absence of UV light, $H_2O_2$ did not have any effect on MDEA degradation for the same period (3 h). The rate of mineralization increased with increasing initial $H_2O_2$ concentrations. The production of hydroxyl radical (•OH) plays an important role in the MDEA mineralization process, which agrees with the similar reported observations [11, 17–19]. Daneshvar et al. [11] reported the enhancement of 4-nitrophenol removal percentage with increasing concentration of hydroxyl radical in the oxidation system. On the other hand, an increase in the rate of degradation of sulfamethoxazole (antibiotic) and the rate of decolorization of Malachite Green with increasing concentrations of $H_2O_2$ have been reported by Behnajady et al. [18] and Lester et al. [19], respectively. Abramović et al. [17] also reported a similar increase in the rate of degradation of thiacloprid (insecticide) with an increase in $H_2O_2$ concentration.

Furthermore, the effect of reaction temperature on the overall mineralization of MDEA can also be seen in Fig. 2. The degree of mineralization was nearly same for all the oxidation temperature up to 30°C indicating that the process in not temperature dependent till $\leq$30°C or nearly the room temperature conditions. This is a good advantage for the future application in which the process oxidation can be conducted at room temperature conditions to achieve maximum efficiency. Meanwhile, an increase in temperature from 30°C up to 50°C had reverse effect on the degree of mineralization, where

© 2013 WILEY-VCH Verlag GmbH & Co. KGaA, Weinheim 

**Table 1.** Estimated reduction rates at initial 30 min

| Temperature (°C) | Experimental | $[C]_0$ (mol $L^{-1}$) | $[H_2O_2]_0$ (mol $L^{-1}$) | $[-d[C]_0/dt]$ (mol $L^{-1}$ $min^{-1}$) | Slope; $R^2$ |
|---|---|---|---|---|---|
| 20 | $[C]_0$ = constant | 0.0847 | 0.0615 | 0.000180 | Slope = 0.5350 |
| | | 0.0847 | 0.0900 | 0.000221 | $R^2$ = 0.9991 |
| | | 0.0851 | 0.1210 | 0.000260 | (Fig. 4) |
| | | 0.0847 | 0.1810 | 0.000317 | |
| | | 0.0852 | 0.2220 | 0.000359 | |
| | $[H_2O_2]_0$ = constant | 0.0432 | 0.2230 | 0.000235 | Slope = 0.5949 |
| | | 0.0852 | 0.2220 | 0.000359 | $R^2$ = 0.9993 |
| | | 0.1280 | 0.2170 | 0.000449 | (Fig. 5) |
| | | 0.1825 | 0.2170 | 0.000556 | |
| 30 | $[C]_0$ = constant | 0.0847 | 0.0615 | 0.000179 | Slope = 0.5354 |
| | | 0.0847 | 0.0900 | 0.000221 | $R^2$ = 0.9991 |
| | | 0.0850 | 0.1210 | 0.000260 | (Fig. 4) |
| | | 0.0847 | 0.1810 | 0.000317 | |
| | | 0.0852 | 0.2230 | 0.000359 | |
| | $[H_2O_2]_0$ = constant | 0.0432 | 0.2220 | 0.000235 | Slope = 0.5947 |
| | | 0.0852 | 0.2230 | 0.000359 | $R^2$ = 0.9993 |
| | | 0.1280 | 0.2170 | 0.000448 | (Fig. 5) |
| | | 0.1825 | 0.2170 | 0.000556 | |
| 40 | $[C]_0$ = constant | 0.0851 | 0.0615 | 0.000144 | Slope = 0.5544 |
| | | 0.0850 | 0.0900 | 0.000178 | $R^2$ = 0.9995 |
| | | 0.0851 | 0.1210 | 0.000210 | (Fig. 4) |
| | | 0.0853 | 0.1800 | 0.000263 | |
| | | 0.0850 | 0.2210 | 0.000290 | |
| | $[H_2O_2]_0$ = constant | 0.0432 | 0.2220 | 0.000194 | Slope = 0.5740 |
| | | 0.0850 | 0.2210 | 0.000290 | $R^2$ = 0.9983 |
| | | 0.1278 | 0.2210 | 0.000370 | (Fig. 5) |
| | | 0.1830 | 0.2210 | 0.000457 | |
| 50 | $[C]_0$ = constant | 0.0848 | 0.0610 | 0.000113 | Slope = 0.5672 |
| | | 0.0848 | 0.0900 | 0.000140 | $R^2$ = 0.9998 |
| | | 0.0850 | 0.1210 | 0.000167 | (Fig. 4) |
| | | 0.0850 | 0.1830 | 0.000210 | |
| | | 0.0850 | 0.2210 | 0.000233 | |
| | $[H_2O_2]_0$ = constant | 0.0432 | 0.2220 | 0.000156 | Slope = 0.5785 |
| | | 0.0850 | 0.2210 | 0.000233 | $R^2$ = 0.9998 |
| | | 0.1280 | 0.2180 | 0.000293 | (Fig. 5) |
| | | 0.1840 | 0.2180 | 0.000361 | |

it decreases with increasing temperature. Most probably when the oxidation temperature is >30°C, hydrogen peroxide ($H_2O_2$) undergoes self-accelerating decomposition. This condition will affect mineralization efficiency. The results obtained are in good agreement with those reported by Kavitha and Palanivelu [20]. They reported that the maximum degradation efficiency of cresol using Fenton's reagent was observed at 30°C and beyond which the degradation efficiency was reported to be constant.

Figure 3 shows the effect of initial concentration of contaminant on the mineralization efficiency at different oxidation temperatures (20–50°C). Four initial concentrations of contaminant ($[C]_0$) in the range of 0.042–0.180 mol $L^{-1}$ were used and initial $H_2O_2$ concentration ($[H_2O_2]_0$), pH, UV intensity, and radiation period were kept constant at 0.22 mol $L^{-1}$, 10.18, 12.06 mW $cm^{-2}$, 3 h, respectively. Based on the trends, it was observed that the mineralization efficiency decrease with increasing initial concentration of contaminant, which is in good agreement with the reported literature [18, 21, 22]. The degradation efficiency was reported to decrease with increasing initial contaminant concentrations. Haji et al. [21] observed that for higher initial concentration of dye with excess $H_2O_2$ took longer time to achieve a specific degradation. On the other hand, Behnajady et al. [18] reported that decolorization decrease with increasing initial concentration of Malachite Green for a constant initial concentration of $H_2O_2$. Ochuma et al. [22] also reported a similar behavior for the degradation rate of 2,4,6-trichlorophenol (TCP). They also concluded that, at constant UV lamp intensity, for the higher concentration of TCP required longer radiation time for complete degradation.

## 3.2 Estimation of hydroxyl radical rate constant on MDEA mineralization

In this study, the degradation/mineralization process was followed by measuring the TOC of the samples during the oxidation process. Based on the MDEA mineralization profile, the MDEA mineralization process can be explained as follows:

$$S + H_2O_2 + h\nu \xrightarrow{k_{exp}} \text{degradation product} \quad (1)$$

© 2013 WILEY-VCH Verlag GmbH & Co. KGaA, Weinheim

CLEAN Soil Air Water

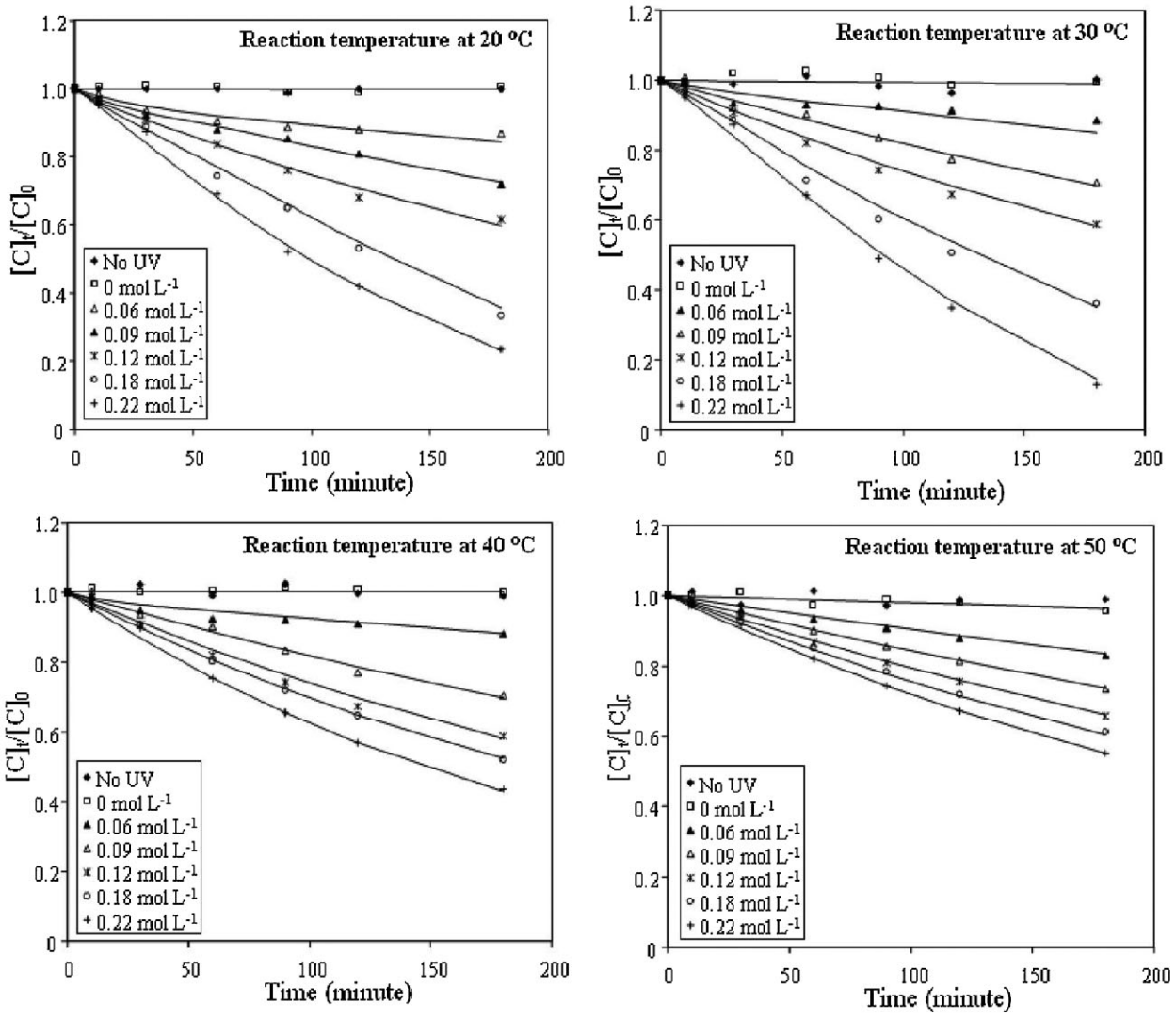


**Figure 2.** MDEA mineralization profile at different initial concentration of $H_2O_2$ ($[H_2O_2]_0$). $[C]_0 = 0.085\,mol\,L^{-1}$ of organic carbon; pH 10.18; UV intensity = 12.06 mW cm$^{-2}$; radiation time = 3 h.

$$H_2O_2 + h\nu \xrightarrow{k_2} 2\,{}^{\bullet}OH \quad (2)$$

$$S + {}^{\bullet}OH \xrightarrow{k_3} \text{degradation products} \quad (3)$$

where S is substrate (MDEA). Hydroxyl radical is well known as a non-selective oxidator. Consequently, the hydroxyl radical react with $H_2O_2$ during oxidation process to produce less reactive radical such as hydroperoxyl radical ($HO_2^{\bullet}$) and $O_2^{\bullet}$, which is known as scavenging reaction. These scavenging reactions during MDEA mineralization may be expressed as follows:

$$H_2O_2 + {}^{\bullet}OH \xrightarrow{k_4} HO_2^{\bullet} + H_2O \quad (4)$$

$$H_2O_2 + {}^{\bullet}OH \xrightarrow{k_5} O_2^{\bullet} + H^+ + H_2O \quad (5)$$

$$H_2O_2 + HO_2^{\bullet} \xrightarrow{k_6} {}^{\bullet}OH + O_2 + H_2O \quad (6)$$

De et al. [12] estimated the hydroxyl radical reaction rate constants for phenol and chlorinated phenols by using UV/$H_2O_2$ photo-oxidation and a similar approach is considered for the mineralization of MDEA. Hence the rate of mineralization $-(d[C]/dt)$ could be estimated as follows:

$$-\frac{d[C]}{dt} = k_3[C][{}^{\bullet}OH] \quad (7)$$

where [C] is the concentration of substrate, [$^{\bullet}$OH] the concentration of hydroxyl radical, and $k_3$ is the hydroxyl radical rate constants for MDEA mineralization. During the oxidation process the scavenging reaction occurs, in which the hydroxyl radicals react with $H_2O_2$ to form other less reactive radicals such as $HO_2^{\bullet}$ and $O_2^{\bullet}$. UV photolysis of $H_2O_2$ (Eq. (2)) and the reaction of $HO_2^{\bullet}$ with $H_2O_2$ (Eq. (6)) leads the formation of $^{\bullet}$OH radical, while the reaction of $^{\bullet}$OH with the substrate (Eq. (3)) and $H_2O_2$ (Eqs. (4) and (5)) leads to the disappearance of $^{\bullet}$OH in the system. Rate of formation of $^{\bullet}$OH by UV photolysis of $H_2O_2$ can be expressed as $\left[\left(\Phi_{H_2O_2} W_{abs,H_2O_2}\right)/V\right]$ [7, 12]. On the other hand, the formation of $HO_2^{\bullet}$ is expressed by Eq. (4) and the disappearance of $HO_2^{\bullet}$ is expressed by Eq. (6). According to the above

© 2013 WILEY-VCH Verlag GmbH & Co. KGaA, Weinheim

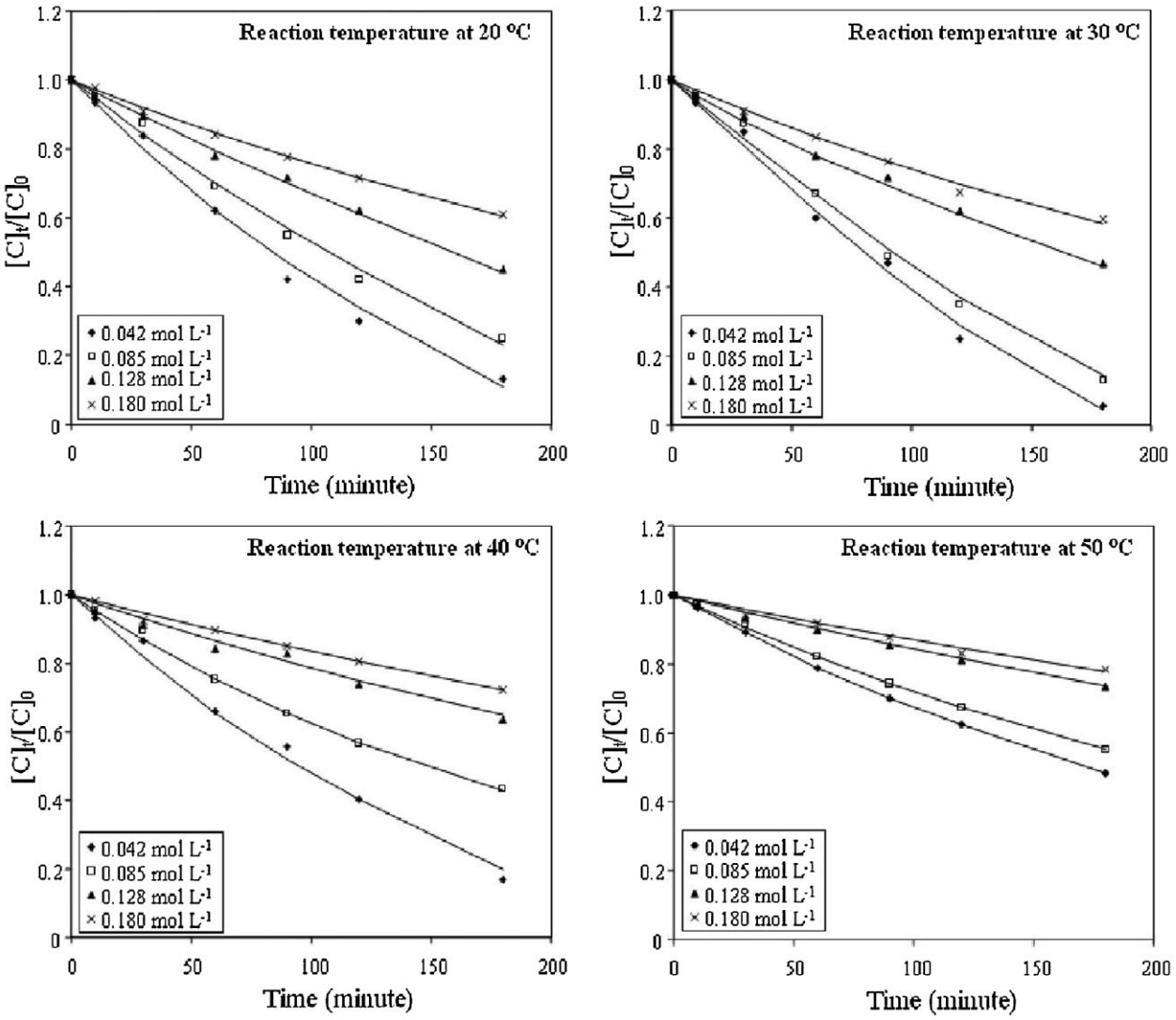


**Figure 3.** MDEA mineralization profile at different initial concentration of contaminant ($[C]_0$) $[H_2O_2]_0 = 0.22\,\text{mol L}^{-1}$; pH 10.18; UV intensity = 12.06 mW cm$^{-2}$; radiation time = 3 h.

reactions, the rate of formation of $^{\bullet}OH$ are $\left[(\Phi_{H_2O_2} W_{abs,H_2O_2})/V\right]$ and $k_6\left[HO_2^{\bullet}\right][H_2O_2]$, according to Eqs. (2) and (6), respectively. Similarly the rate of disappearance of $^{\bullet}OH$ can be represented as $-k_3[C][^{\bullet}OH]$, $-k_4[H_2O_2][^{\bullet}OH]$, and $-k_5[^{\bullet}OH][H_2O_2]$, according to Eqs. (3)–(5), respectively. Hence, the net rate of formation can be represented as follows:

$$\frac{d[^{\bullet}OH]}{dt} = \left[\frac{\Phi_{H_2O_2} W_{abs,H_2O_2}}{V}\right] + k_6[HO_2^{\bullet}][H_2O_2] - k_3[C][^{\bullet}OH] - k_4[H_2O_2][^{\bullet}OH] - k_5[^{\bullet}OH][H_2O_2] \quad (8)$$

where $\Phi_{H_2O_2}$ is the quantum yields of the photolysis of $H_2O_2$ (mol/E), $W_{abs,H_2O_2}$ is the radiation flow rate absorbed by $H_2O_2$ (E/s), and $V$ is the volume of solution irradiated (L). Similarly the net rate of formation of $HO_2^{\bullet}$ can be estimated from the rate of formation (Eq. (4)) and disappearance (Eq. (6)), respectively:

$$\frac{d[HO_2^{\bullet}]}{dt} = k_4[H_2O_2][^{\bullet}OH] - k_6\left[HO_2^{\bullet}\right][H_2O_2] \quad (9)$$

where $[HO_2^{\bullet}]$ and $[^{\bullet}OH]$ are the concentrations of $HO_2^{\bullet}$ and $^{\bullet}OH$, respectively, and $k_3$, $k_4$, $k_5$, and $k_6$ are the rate constants. The species involved in the reactions namely $[^{\bullet}OH]$ and $[HO_2^{\bullet}]$ are the intermediates and are very reactive and do not accumulate during the reaction. After the induction period, the steady state approximation assumes that the rate of formation of the individual species ($[^{\bullet}OH]$ and $[HO_2^{\bullet}]$) is equal to the rate of disappearance [1, 3, 12, 19, 23, 29] and hence, $(d[^{\bullet}OH]/dt) = 0$ and $(d[HO_2^{\bullet}]/dt) = 0$. Using this steady state conditions, an equation for $[^{\bullet}OH]$ can be derived, by rearranging Eq. (9) and then substituting into Eq. (8) to yield:

$$[^{\bullet}OH] = \frac{\left[(\Phi_{H_2O_2} W_{abs,H_2O_2})/V\right]}{k_3[C] + k_5[H_2O_2]} \quad (10)$$

Further substituting Eq. (10) into Eq. (7) yields:

$$-\frac{d[C]}{dt} = k_3[C]\frac{\left[(\Phi_{H_2O_2} W_{abs,H_2O_2})/V\right]}{k_3[C] + k_5[H_2O_2]} \quad (11)$$

© 2013 WILEY-VCH Verlag GmbH & Co. KGaA, Weinheim

During the start of the reaction (time, $t \approx 0$), the reaction of $H_2O_2$ scavenging to hydroxyl radical ($^{\bullet}OH$) can be neglected (Eqs. (4) and (5)) and hence, the initial mineralization rate $-(d[C]_0/dt)$ is equal to the rate of formation of hydroxyl radical $d[^{\bullet}OH]/dt$ by UV photolysis of $H_2O_2$ as represented in Eq. (2). The generation rate of hydroxyl radical at the initial time without any scavenging can be expressed as $\left[(\Phi_{H_2O_2} W_{abs,H_2O_2})/V\right]$ [12], therefore:

$$-\frac{d[C]_0}{dt} = \left[\frac{\Phi_{H_2O_2} W_{abs,H_2O_2}}{V}\right]$$

and hence Eq. (11) can be modified as:

$$-\frac{d[C]}{dt} = k_3[C]\frac{-d[C]_0/dt}{k_3[C] + k_5[H_2O_2]} \quad (12)$$

The initial rate equation can be expressed as [24]:

$$-\frac{d[C]_0}{dt} = k_{exp.}[C]_0^a[H_2O_2]_0^b \quad (13)$$

where $k_{exp}$ is the mineralization rate constant observed and $t$ is the oxidation time. Further, 'a' and 'b' are the order of reactions. By combining and rearranging Eqs. (12) and (13), the mineralization rate can be expressed as:

$$\left[\frac{[C]_0^a[H_2O_2]_0^b}{-d[C]/dt}\right] = \frac{1}{k_{exp}} + \frac{k_5}{k_{exp}k_3}\left[\frac{[H_2O_2]}{[C]}\right] \quad (14)$$

Furthermore, the order of reaction ('a' and 'b') may be calculated by initial rate method [24] by using Eq. (13). For the estimation of the order of reaction 'b', the experiments were conducted at five different concentrations of $H_2O_2$ at constant initial concentration of substrate $[C]_0$. Based on the above condition, the logarithmic form of Eq. (13) is:

$$\ln\left[-\frac{d[C]_0}{dt}\right] = \ln k' + b\ln[H_2O_2]_0 \quad (15)$$

where $k' = k_{exp}[C]_0^a$. The present experimental results (Tab. 1) were used to estimate the order of reaction 'b' by plotting $\ln[-d[C]_0/dt]$ versus $\ln[H_2O_2]_0$ (Fig. 4) and the estimated slope was approximately 0.55 at four different reaction temperatures (20, 30, 40, and 50°C). Similarly for the estimation of 'a' the experiments were conducted at four different initial concentration of substrate $[C]_0$ by keeping the initial concentration of $[H_2O_2]_0$ at constant. A plot $\ln[-d[C]_0/dt]$ versus $\ln[C]_0$ shows a linear correlation, as shown in Fig. 5, and the estimated slope was approximately 0.58 at all reaction temperatures tested. Using the estimated values for 'a' and 'b', Eq. (13) becomes:

$$-\frac{d[C]_0}{dt} = k_{exp.}[C]_0^{0.58}[H_2O_2]_0^{0.55} \quad (13)$$

indicating that the overall mineralization process at the initial reaction time follows the pseudo first order reaction. Based on the experimental rate equation (Eq. (13)), it can be shown that the mineralization rate depends on both $[C]_0$ and $[H_2O_2]_0$ where $[C]_0$ is slightly dominant than $[H_2O_2]_0$. This may be due to the presence of intermediate products such as organic acids which cannot be readily degradable by hydroxyl radical. Therefore, due to the scavenging reaction the concentration of hydroxyl radical in the system decreased. Thus, the MDEA mineralization process was dominantly controlled by $[C]_0$.

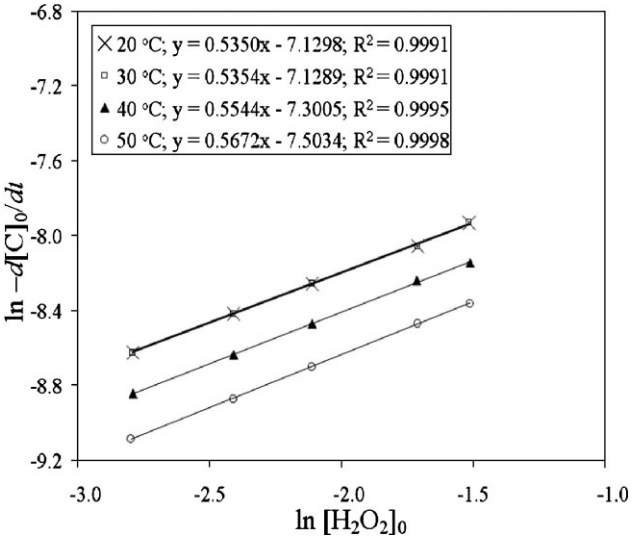


**Figure 4.** Plot of $\ln[-d[C]_0/dt]$ versus $\ln[H_2O_2]_0$ at four different temperatures and pH 10.18.

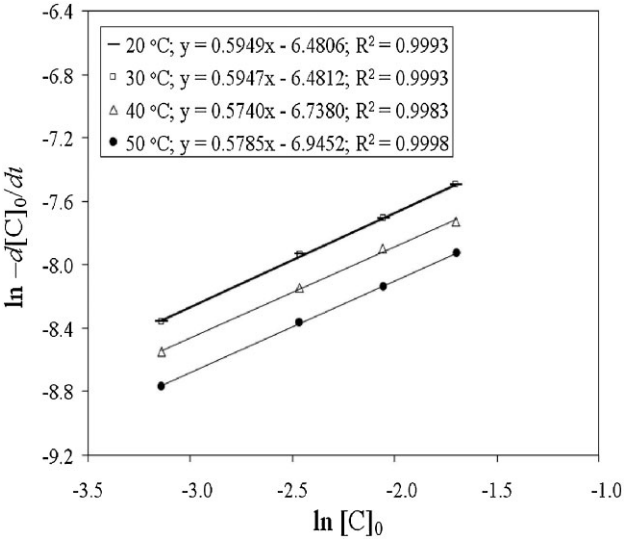


**Figure 5.** Plot of $\ln[-d[C]_0/dt]$ versus $\ln[C]_0$ at four different temperature and pH 10.18.

According to De et al. [25], the reaction rate of second stage of phenol degradation by UV/$H_2O_2$ was interfered by organic acid formed in the system. The formation of organic acid reduced the concentration of hydroxyl radical in the system. Therefore the reaction rate was controlled by the concentration of phenol available in the reaction medium [25]. Similarly acetic, maleic, and oxalic acid are the organic acids that are not readily degradable by hydroxyl radical, Jone [5] and Koprivanac and Kusic [6]. Hence, the incomplete of MDEA mineralization might be attributed to the formation of acidic intermediate products that are not readily degradable by hydroxyl radical.

On the other hand, the present experimental results (Tab. 1) were used for solving Eq. (14) and the plot is shown in Fig. 6. For the

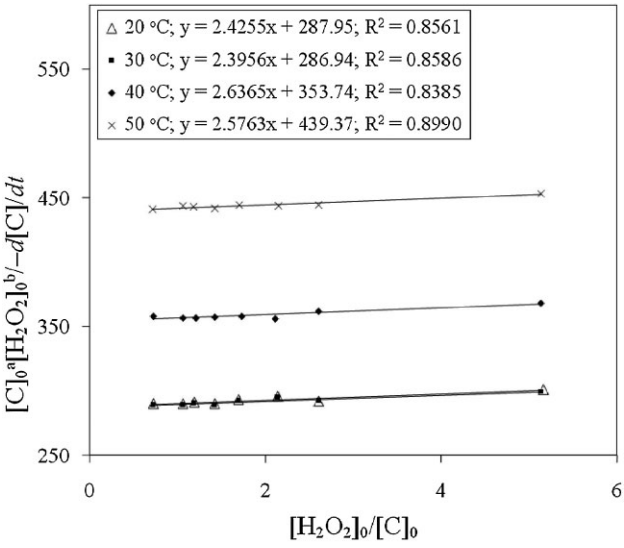


**Figure 6.** Plot of $[C]_0^a[H_2O_2]_0^b/-d[C]/dt$ versus $[H_2O_2]_0/[C]_0$ (Eq. (14)) at four different temperatures and pH 10.18.

estimation of kinetic constants, the reported value for $k_5$ at pH 10.5 = $30 \times 10^7$ L mol$^{-1}$ s$^{-1}$ was considered [26] and the rate of substrate degradation for the reaction at the first 30 min $[-d[C]_0/dt]$ was calculated from the experimental data (Tab. 1) for each experimental condition. The results are summarized in Tab. 2. The estimated hydroxyl radical rate constants are similar at 20 and 30°C of the oxidation process. As discussed earlier based on the mineralization profile of MDEA, the oxidation process is not dependent on temperature up to 30°C. Above 30°C, the hydroxyl radical rate constants ($k_3$) increased from $2.14 \times 10^{11}$ L mol$^{-1}$ min$^{-1}$ at 30°C to $3.07 \times 10^{11}$ L mol$^{-1}$ min$^{-1}$ at 50°C ($3.57 \times 10^9$ L mol$^{-1}$ s$^{-1}$ at 30°C to $5.12 \times 10^9$ L mol$^{-1}$ s$^{-1}$). Theoretically, this condition will result in an increase in TOC removal, when the oxidation is conducted at higher temperatures, but in fact the raise in temperature decreases the organic carbon removal ($k_{exp}$ decreased from $3.47 \times 10^{-3}$ L mol$^{-1}$ min$^{-1}$ at 30°C to $2.28 \times 10^{-3}$ L mol$^{-1}$ min$^{-1}$ at 50°C), which might be due to the reason that, an increase in oxidation temperature resulted in increasing the scavenging reaction as well, which in turn reduces the concentration of hydroxyl radical in the system. Also, by increasing of oxidation temperature, $H_2O_2$ tend to undergo self-accelerating decomposition. For the comparison, De et al. [12] reported the estimated hydroxyl radical rate constants as $1 \times 10^{10}$ g mol$^{-1}$ s$^{-1}$ for the degradation of 2- and 4-chlorophenol using UV/$H_2O_2$ in aqueous solution at room temperature. For the case of monoethanolamine (MEA) using Fenton's reagent at room temperature the reported hydroxyl radical rate constant was $2.9 \times 10^6$ M$^{-1}$ min$^{-1}$ ($4.8 \times 10^4$ M$^{-1}$ s$^{-1}$) [1]. Based on these results reported by De et al. [12] and Harimurti et al. [1], the present estimated hydroxyl radical rate constants for the mineralization of MDEA by using UV/$H_2O_2$ is smaller compared to the reported rate constants for aromatic compounds such as phenol, but the present estimated values are higher compared to those obtained using Fenton treatment for the oxidation of same group of compound, i.e., monoethanolamine. Table 3 presents the comparison of the reported hydroxyl radical rate constants for different pollutants using various methods of oxidation process. The present

**Table 2.** Calculated values for $k_{exp}$ and $k_3$

| $T$ (°C) | $T$ (K) | $1/T$ | $1/k_{exp}$ | Slope (Eq. (14)) | $k_{exp}$ (M$^{-1}$ min$^{-1}$) | $k_3$ (M$^{-1}$ min$^{-1}$) | ln$k_3$ |
|---|---|---|---|---|---|---|---|
| 20 | 293 | 0.0034 | 287.95 | 2.4255 | 0.003473 | $2.14 \times 10^{11}$ | 26.08780 |
| 30 | 303 | 0.0033 | 286.94 | 2.3956 | 0.003485 | $2.16 \times 10^{11}$ | 26.09669 |
| 40 | 313 | 0.0032 | 353.74 | 2.6365 | 0.002827 | $2.42 \times 10^{11}$ | 26.21016 |
| 50 | 323 | 0.0031 | 439.37 | 2.5763 | 0.002276 | $3.07 \times 10^{11}$ | 26.45004 |

**Table 3.** Reported values for hydroxyl radical rate constants for different compounds

| Process | Method | Rate constants | References |
|---|---|---|---|
| Degradation of: | UV/$H_2O_2$ | | [12] |
| Phenol | | $(1.41 \pm 0.6) \times 10^{10}$ g mol$^{-1}$ s$^{-1}$ | |
| 2-Chlorophenols | | $(9.10 \pm 2.1) \times 10^{10}$ g mol$^{-1}$ s$^{-1}$ | |
| 4-Chlorophenols | | $(1.07 \pm 0.4) \times 10^{10}$ g mol$^{-1}$ s$^{-1}$ | |
| Degradation of methyl *tert*-butyl ether (MTBE) | UV/$H_2O_2$ | $(3.9 \pm 0.73) \times 10^9$ M$^{-1}$ s$^{-1}$ = $(3.9 \pm 0.73) \times 10^9$ L mol$^{-1}$ s$^{-1}$ | [32] |
| Degradation of 4-chloro-3,5-dinitrobenzoic acid | UV/$H_2O_2$ | $3.5 \times 10^9$ L mol$^{-1}$ s$^{-1}$ | [13] |
| Degradation of carbendazim | UV/$H_2O_2$ | $(2.2 \pm 0.3) \times 10^9$ M$^{-1}$ s$^{-1}$ = $(2.2 \pm 0.3) \times 10^9$ L mol$^{-1}$ s$^{-1}$ | [31] |
| Degradation of sulfamethoxazole | UV/$H_2O_2$ | $(3.5–6.8) \times 10^9$ M$^{-1}$ s$^{-1}$ = $(3.5–6.8) \times 10^9$ L mol$^{-1}$ s$^{-1}$ | [19] |
| Mineralization of monoethanolamine | UV/$H_2O_2$ | $(4.7–15) \times 10^{10}$ M$^{-3}$ s$^{-1}$ = $(4.7–15) \times 10^{10}$ L$^3$ mol$^{-3}$ s$^{-1}$ | [4] |
| Mineralization of monoethanolamine | Fenton's reagent | $2.9 \times 10^6$ M$^{-1}$ min$^{-1}$ = $4.8 \times 10^4$ M$^{-1}$ s$^{-1}$ = $4.8 \times 10^4$ L mol$^{-1}$ s$^{-1}$ | [1] |
| Mineralization of di-isopropanolamine | Fenton's reagent | $1.43 \times 10^7$ M$^{-1}$ min$^{-1}$ = $2.38 \times 10^5$ M$^{-1}$ s$^{-1}$ = $2.38 \times 10^5$ L mol$^{-1}$ s$^{-1}$ | [3] |
| Mineralization of methyldiethanolamine | UV/$H_2O_2$ | | Present work |
| At 20°C | | $2.14 \times 10^{11}$ L mol$^{-1}$ min$^{-1}$ = $3.57 \times 10^9$ L mol$^{-1}$ s$^{-1}$ | |
| At 30°C | | $2.16 \times 10^{11}$ L mol$^{-1}$ min$^{-1}$ = $3.60 \times 10^9$ L mol$^{-1}$ s$^{-1}$ | |
| At 40°C | | $2.42 \times 10^{11}$ L mol$^{-1}$ min$^{-1}$ = $4.03 \times 10^9$ L mol$^{-1}$ s$^{-1}$ | |
| At 50°C | | $3.07 \times 10^{11}$ L mol$^{-1}$ min$^{-1}$ = $5.12 \times 10^9$ L mol$^{-1}$ s$^{-1}$ | |

© 2013 WILEY-VCH Verlag GmbH & Co. KGaA, Weinheim

CLEAN Soil Air Water

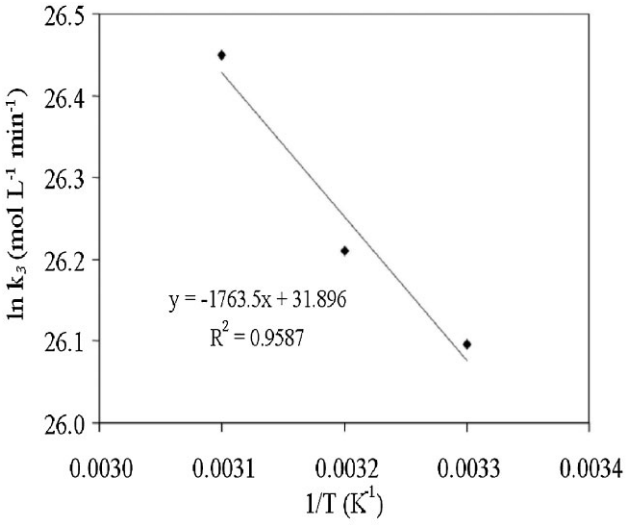


**Figure 7.** Plot of $\ln k_3$ versus $1/T$.

estimated values are satisfactorily comparable with those reported in the literature.

## 3.3 Temperature dependence on mineralization of MDEA

In the present study, the experiments on the mineralization of MDEA by UV/$H_2O_2$ were conducted at four different temperatures ranging from 20 to 50°C, since the optimum oxidation temperature was found within this range. The activation energy of a reaction can be calculated using Arrhenius' law [23, 27, 28]:

$$k = A_0 e^{-Ea/RT} \tag{16}$$

where $k$ = hydroxyl radical reaction rate constant; $A_0$ = Arrhenius $A$ factor; $Ea$ = activation energy; $R$ = ideal gas constant = 8.314 J K$^{-1}$ mol$^{-1}$; $T$ = temperature (K). The logarithmic form of Eq. (16) can be written as:

$$\ln k = \ln A_0 - \frac{Ea}{R}\frac{1}{T} \tag{17}$$

The rate constants of hydroxyl radical oxidation at temperature 20 and 30°C were found to be similar. Hence, the activation energies were calculated using the rate constants from 30 to 50°C. Using the present calculated data (Tab. 2) a plot of $\ln k_3$ versus $1/T$ (Fig. 7) was made and the activation energy was estimated using the estimated value for the slope, and the activation energy thus estimated is 14.66 kJ mol$^{-1}$. Table 4 compares the reported activation energy values for the hydroxyl radical oxidation process for different pollutants. The present estimated activation energy 14.66 kJ mol$^{-1}$ obtained for the mineralization of MDEA is in the similar range and comparable with the reported activation energy on hydroxyl radical degradation for simple phenolic compounds such as *ortho*-, *metha*-, and *para*-cresol [20], and slightly less than that reported for complex phenolic compounds such as 2,4,6-trichlorophenol [22], *p*-hydroxybenzoic acid [29], and 2,4-dichlorophenoxyacetic acid [30] which might also be attributed to the type of oxidation process involved.

## 3.4 Energy efficiency estimations

Economics factor is often to be more paramount during the selection of wastewater treatment technology rather than regulations, effluent goals, and operations (maintenance, control, safety), Daneshvar et al. [33]. Since the UV/$H_2O_2$ process for mineralization of MDEA is an electric-energy-intensive process and the electric energy can represent major consumption cost, then the estimation of electrical energy demand is essential. Legrini et al. [34] proposed a general and simple method for the evaluation of electrical energy for AOPs. The evaluation of electrical energy was thus represented as energy efficiency, while the efficiencies was expressed as the ratio of ppm TOC destroyed to electrical power consumed during the time of irradiation. After the multiplication with the total volume of solution treated, then the calculation results in efficiency which is independent of equipment size. The energy efficiency that was proposed is expressed in Eq. (17):

$$\phi = \frac{\Delta \mathrm{TOC} \times V}{P} \tag{17}$$

where $\phi$ is the energy efficiency, ΔTOC the total organic carbon destroyed (ppm), $V$ the total volume of solution treated (L), and $P$ is the electrical power consumed (kW h). Based on these the calculated energy efficiency of MDEA mineralization in the present work was estimated as 14.29 g kW h$^{-1}$, whereas the reported energy efficiency of MDEA mineralization using ZnO/$SnO_2$ coupled with photocatalysts as reported as 0.77 g kW h$^{-1}$, Ali et al. [35]. The estimated values are compared in Tab. 5, which show the energy efficiency of the present process.

**Table 4.** Activation energy of hydroxyl radical oxidation for different pollutants

| Process | Method | Activation energy (kJ mol$^{-1}$) | References |
|---|---|---|---|
| Degradation of *p*-hydroxybenzoic acid | UV/Fenton's reagent | 32.8 | [29] |
| Degradation of 2,4-dichlorophenoxyacetic acid | Anodic Fenton | 26.1 ± 0.9 | [30] |
| Destruction of: | Fenton's reagent | | [20] |
| *o*-Cresol | | 16.25 | |
| *m*-Cresol | | 12.90 | |
| *p*-Cresol | | 14.95 | |
| Photocatalytic oxidation of 2,4,6-trichlorophenol | UV/$O_2$/$TiO_2$ | 19.98 | [22] |
| Degradation of formaldehyde | UV-Fenton | 9.85 | [33] |
| Mineralization of methyldiethanolamine | UV/$H_2O_2$ | 14.66 | Present work |

© 2013 WILEY-VCH Verlag GmbH & Co. KGaA, Weinheim

**Table 5.** Comparison of energy efficiency of MDEA mineralization in the present work and MDEA mineralization using $ZnO/SnO_2$ coupled photocatalysts

| AOP method | Experimental | ΔTOC (ppm) | $\phi$ (g kW h$^{-1}$) | References |
|---|---|---|---|---|
| $ZnO/SnO_2$ coupled photocatalysts | $[MDEA]_0 = 1000$ ppm<br>$[TOC]_0 = 503.53$ ppm<br>$V = 0.25$ L<br>UV lamp = 12 W (365 nm)<br>Irradiation time = 3 h<br>ΔTOC at 3 h reaction = 22% | 110.76 | 0.77 | [36] |
| $UV/H_2O_2$ | [MDEA]0 = 2000 ppm<br>$[TOC]_0 = 1006$ ppm<br>$V = 0.4$ L<br>UV lamp = 8 W LP Hg lamp (254 nm)<br>Irradiation time = 3 h<br>ΔTOC at 3 h reaction = 85.74% | 857.4 | 14.29 | Present work |

## 4 Conclusions

Hydroxyl radical is the important species in the MDEA mineralization. The order of reaction was found to be independent of temperature. The reaction rate constant of hydroxyl radical oxidation was nearly constant at oxidation temperature at 20 and 30°C and beyond which it increases with increasing temperature. Activation energy of MDEA mineralization by hydroxyl radical was found to be 14.66 kJ mol$^{-1}$. The estimated energy efficiency show a better performance of the present process, when compared with the mineralization of MDEA, using $ZnO/SnO_2$ coupled with photocatalysts. The present estimated rate constants and the activation energy for the MDEA mineralization will be of useful for the design and scale up of commercial process for the treatment of MDEA present in the effluent streams.

### Acknowledgments

The authors are thankful to Universiti Teknologi PETRONAS for financial support.

*The authors have declared no conflict of interest.*

## References

[1] S. Harimurti, B. K. Dutta, I. F. B. M. Ariff, S. Chakrabarti, D. Vione, Degradation of Monoethanolamine in Aqueous Solution by Fenton's Reagent with Biological Post-Treatment, *Water Air Soil Pollut.* **2010**, *211 (1–4)*, 273–286.

[2] B. K. Dutta, S. Harimurti, I. F. B. M. Ariff, S. Chakrabarti, D. Vione, Degradation of Diethanolamine by Fenton's Reagent Combined with Biological Post-Treatment, *Desalin. Water Treat.* **2010**, *19 (1–3)*, 286–293.

[3] A. A. Omar, R. M. Ramli, P. N. F. M. Khamarudin, Fenton Oxidation of Natural Gas Plant Wastewater, *Can. J. Chem. Eng. Technol.* **2010**, *1*, 1–6.

[4] I. F. B. M. Ariff, *MSc Thesis*, Universiti Technology PETRONAS, Malaysia **2010**.

[5] C. W. Jones, *Application of Hydrogen Peroxide and Derivatives*, RSC Clean Technology Monographs, Formerly of Solvay Interox R&D, Widnes, UK **1999**.

[6] N. Koprivanac, H. Kusic, *AOP as an Effective Tool for The Minimization of Hazarduce Organic Pollutants in Colored Wastewater; Chemical and Photochemical Processes, Hazardous Material and Wastewater*, Nova Science Publisher, Hauppauge, NY **2007**, pp. 149–199.

[7] T. Oppenländer, *Photochemical Purification of Water and Air*, Wiley-VCH, Weinheim **2003**.

[8] W. Z. Tang, *Physicochemical Treatment of Hazardous Waste*, Lewis Publisher, Boca Raton, FL **2004**.

[9] P. K. Malik, S. K. Sanyal, Kinetics of Decolourisation of Azo Dyes in Water by $UV/H_2O_2$ Process, *Sep. Purif. Technol.* **2004**, *36*, 167–175.

[10] M. Muruganandham, M. Swaminathan, Photochemical Oxidation of Reactive Azo Dye with $UV–H_2O_2$ Process, *Dyes Pigm.* **2004**, *62*, 269–275.

[11] N. Daneshvar, M. A. Behnajady, Y. Z. Asghar, Photooxidative Degradation of 4-Nitrophenol (4-NP) in $UV/H_2O_2$ Process: Influence of Operational Parameters and Reaction Mechanism, *J. Hazard. Mater.* **2007**, *B139*, 275–279.

[12] A. K. De, B. Chaudhuri, S. Bhattacharjee, B. K. Dutta, Estimation of $^{\bullet}OH$ Radical Reaction Rate Constants for Phenol and Chlorinated Phenols Using $UV/H_2O_2$ Photo-Oxidation, *J. Hazard. Mater.* **1999**, *B64*, 91–104.

[13] J. L. Lopez, F. S. G. Einschlag, M. C. Gonzáles, A. L. Capparelli, E. Oliveros, T. M. Hashem, A. M. Braun, Hydroxyl Radical Initiated Photodegradation of 4-Chloro-3,5-dinitrobenzoic Acid in Aqueous Solution, *J. Photochem. Photobiol., A* **2000**, *137*, 177–184.

[14] P. Kajitvichyanukul, M.-C. Lu, C.-H. Liao, W. Wirojanagud, T. Koottapep, Degradation and Detoxification of Formalin Wastewater by Advanced Oxidation Processes, *J. Hazard. Mater.* **2006**, *B135*, 337–343.

[15] J. Mendham, R. C. Denney, J. D. Barnes, M. J. K. Thomas, *Vogel's Textbook of Quantitative Chemical Analysis*, 6th Ed., Prentice Hall, Upper Saddle River, NJ **2000**.

[16] S. Harimurti, A. U. Rahmah, A. A. Omar, T. Murugesan, Application of Response Surface Method in the Degradation of Wastewater Containing MDEA Using $UV/H_2O_2$ Advance Oxidation Process, *J. Appl. Sci.* **2012**, *12 (11)*, 1093–1099.

[17] B. F. Abramović, N. D. Banić, D. V. Šojić, Degradation of Thiacloprid in Aqueous Solution by UV and $UV/H_2O_2$ Treatments, *Chemosphere* **2010**, *81*, 114–119.

[18] M. A. Behnajady, N. Modishahla, M. Shokri, B. Vahid, Investigation of the Effect of Ultrasonic Wave on the Enhancement of Efficiency of Direct Photolysis and Photooxidation Processes on the Removal of A Model Contaminant from Textile Industry, *Global NEST J.* **2008**, *10 (1)*, 8–15.

[19] Y. Lester, D. Avisar, H. Mamane, Photodegradation of Antibiotic Sulphamethoxazole in Water with $UV/H_2O_2$ Advanced Oxidation Process, *Environ. Technol.* **2010**, *31 (2)*, 175–183.

[20] V. Kavitha, K. Palanivelu, Destruction of Cresols by Fenton Oxidation Process, *Water Res.* **2005**, *39*, 3062–3072.

[21] S. Haji, B. Benstaali, N. Al-Bastaki, Degradation of Methyl Orange by $UV/H_2O_2$ Advanced Oxidation Process, *Chem. Eng. J.* **2011**, *168*, 134–139.

[22] I. J. Ochuma, R. P. Fishwick, J. Wood, J. M. Winterbottom, Photocatalytic Oxidation of 2,4,6-Trichlorophenol in Water Using a Cocurrent Downflow Contactor Reactor (CDCR), *J. Hazard. Mater.* **2007**, *144*, 627–633.

[23] I. R. Levine, *Physical Chemistry*, 6th Ed., McGraw Hill, New York **2009**.

© 2013 WILEY-VCH Verlag GmbH & Co. KGaA, Weinheim

[24] K. Y. Li, C. C. Liu, Q. Ni, Z. F. Liu, F. Y. C. Huang, Colapret, Kinetic Study of UV Peroxidation of Bis(2-chloroethyl) Ether in Aqueous Solution, *Ind. Eng. Chem. Res.* **1995**, *34*, 1960–1968.

[25] A. K. De, S. Bhattacharjee, B. K. Dutta, Kinetics of Phenol Photooxidation by Hydrogen Peroxide and Ultraviolet Radiation, *Ind. Eng. Chem. Res.* **1997**, *36*, 3607–3612.

[26] H. Christensen, K. Sehested, H. Corfitzen, Reaction of Hydroxyl Radical with Hydrogen Peroxide at Ambient and Elevated Temperatures, *J. Phys. Chem.* **1982**, *86 (9)*, 1588–1590.

[27] O. Levenspiel, *Chemical Reaction Engineering*, 3rd Ed., John Wiley & Sons, Hoboken, USA **1999**.

[28] H. S. Fogler, *Elements of Chemical Reaction Engineering*, 4th Ed., Prentice Hall, Upper Saddle River, NJ **2006**.

[29] J. Beltran, J. Torregrosa, J. R. Domiguez, J. A. Peres, Advanced Oxidation Processes for the Degradation of *p*-Hydroxybenzoic Acid 2: Photo-assisted Fenton Oxidation, *J. Chem. Technol. Biotechnol.* **2001**, *76*, 1243–1248.

[30] Q. Wang, A. T. Lemley, Kinetic Model and Optimization of 2,4-D Degradation by Anodic Fenton Treatment, *Environ. Sci. Technol.* **2001**, *35*, 4509–4514.

[31] P. Mazellier, É. Leroy, J. De Laat, B. Legube, Degradation of Carbendazim by UV/$H_2O_2$ Investigated by Kinetic Modeling, *Environ. Chem. Lett.* **2003**, *1*, 68–72.

[32] P. B. L. Chang, T. M. Young, Kinetics of Methyl *tert*-Butyl Ether Degradation and By-Product Formation during UV/Hydrogen Peroxide Water Treatment, *Water Res.* **2000**, *38 (8)*, 2233–2240.

[33] X. Liu, J. Liang, X. Wang, Kinetics and Reaction Pathways of Formaldehyde Degradation Using the UV-Fenton Method, *Water Environ. Res.* **2011**, *83 (5)*, 418–426.

[34] N. Daneshvar, A. Aleboyeh, A. R. Khataee, The Evaluation of Electrical Energy per Order (EEO) for Photooxidative Decolorization of Four Textile Dye Solution by The Kinetic Model, *Chemosphere* **2005**, *59*, 761–767.

[35] O. Legrini, E. Oliveros, A. M. Braun, Photochemical Process for Water Treatment, *Chem. Rev.* **1993**, *93*, 671–698.

[36] R. Ali, W. A. W. Abu Bakar, S. S. Mislan, M. A. Sharifuddin, Photodegradation of *N*-Methyldiethanolamine over ZnO/SnO2 Coupled Photocatalysts, *Sci. Iran. Trans. C* **2010**, *17 (2)*, 124–130.

© 2013 WILEY-VCH Verlag GmbH & Co. KGaA, Weinheim 